Rare Metal Materials and Engineering
Volume 48, Issue 1, January 2019
Available online at www.rmme.ac.cn

Science Press

Cite this article as: Rare Metal Materials and Engineering, 2019, 48(1): 0024-0032.

ARTICLE

Microstructure Evolution of Semi-solid $TiAl_3$/A356 Composite Prepared by Ultrasonic Vibration

Sun Yonghui[1], Yan Hong[1], Chen Xiaohui[2], Wan Jun[1], Yu Baobiao[1]

[1] Nanchang University, Nanchang 330031, China; [2] Xinyu University, Xinyu 338004, China

Abstract: The semi-solid $TiAl_3$/A356 aluminum composite was prepared by ultrasonic vibration treatment (UVT). The effects of UVT temperature, time and power on the microstructure of semi-solid slurry of $TiAl_3$/A356 composite were studied by SEM and XRD. The results reveal that the size of primary α-Al particles increases with the decrease of UVT temperature and power. The size of the primary α-Al particle decreases first and then increases with the increase of UVT time. When treated at a UVT temperature of 608 °C and a UVT power of 1 kW for 60 s, a good primary α-Al particle morphology with an average size of 62 μm and a shape coefficient of 0.8 can be obtained. The mechanism involved in the development of microstructure is the result of the increase of nucleation rates and undercooling caused by cavitation and acoustic streaming. Furthermore, the in situ $TiAl_3$ particles have strong ability to nucleate α-Al particles.

Key words: microstructure; semi-solid; aluminum matrix composite; ultrasonic vibration; primary α-Al particle

In recent years, aluminum alloys have been widely used in various fields due to their good plasticity and other advantages[1-3]. Lots of earlier scholars[4-6] have focused on the preparation of aluminum alloy and they pointed out that these materials exhibit a dramatically high tensile strength and yield strength. Nevertheless, the poor toughness, low hardness and other weaknesses of aluminum alloy still exist. To satisfy higher requirements, a great deal of work[7-9] has been devoted to the preparation aluminum matrix composites. These studies revealed that properties such as tensile and bending strength, cracking resistance can be significantly improved by particle reinforcements, but the microstructure can hardly be changed and grains are still coarse. To solve the problem, modification treatment has been widely used to obtain refined grains.

Among these structural engineering materials, metal-matrix composites (MMCs) have attracted lots of attentions for a long time. MMCs consist normally of a metallic matrix and a ceramic reinforcement in the form of particles, whiskers or fibres. Wang et al[10] successfully prepared Al-12Si matrix composites reinforced with Ti-Al-based particles and the tensile properties of the composites were effectively improved by the addition of the reinforcing Ti-Al-Nb-Mo-B (TNM) crystalline particles. In situ $TiAl_3$ particles reinforced aluminum MMCs has a high degree of promise due to their good interfacial properties. However, it is difficult to disperse the exogenously formed $TiAl_3$ particles into an aluminum melt. Hence, in this study, in situ formed $TiAl_3$ particles reinforced aluminum MMCs were successfully prepared by a fluoride flux assisting method. Few studies have prepared MMCs in this way. As shown in reaction (1), $TiAl_3$ is produced by the reaction of aluminum melt and K_2TiF_6 powders. The in situ fabrication technique for MMCs can be easily adapted by conventional processes.

$$3K_2TiF_6+13Al=3TiAl_3+2(3KF\cdot AlF_3)+2AlF_3 \quad (1)$$

What's more, some other methods such as up grading preparation techniques are used to obtain refined grains. The semi-solid metal forming technique has developed into one of the most promising forming techniques in the 21st century due to its many advantages compared with conventional processes. Since then, semi-solid metal forming technique has further matured, and the preparation of semi-solid metal features a variety of methods, such as

Received date: December 24, 2017
Foundation item: National Natural Science Foundation of China (51364035); Natural Science Foundation of Jiangxi Province (20171BAB206034)
Corresponding author: Yan Hong, Ph. D., Professor, Department of Materials Processing Engineering, School of Mechanical and Electrical Engineering, Nanchang University, Nanchang 330031, P. R. China, Tel: 0086-791-83969633, E-mail: yanhong_wh@163.com

mechanical stirring [11-14], electromagnetic stirring [15], and UVT [16-18]. UVT in its simplicity, security, and other characteristics considerable attention has gained. For example, a recently study[19] indicated that finer Mg_2Si particles are distributed uniformly in semi-solid magnesium alloy due to the strong transient cavitation and acoustic streaming induced by UVT. Therefore, UVT may be also effective to disperse other particles in semi-solid composite. Thus, in this work, the semi-solid $TiAl_3$/A356 aluminum matrix composite prepared by UVT were studied. The effects of some key ultrasonic parameters on the development of microstructure were investigated, such as temperature, time and power of UVT. Besides, the mechanism of grain refinement was also discussed.

1 Experiment

Materials in this experiment consisted of A356 alloy (Si 7, Mg 0.35, Al balance, wt%) and K_2TiF_6 powder (purity> 99.5%). The liquidus temperature of the composite is 615 °C. First, K_2TiF_6 powders were baked at 250 °C for 2.5 h to remove the crystal water. A356 alloy was overheated to 740 °C in a resistance furnace. Then K_2TiF_6 powders wrapped with aluminum foil were added to the melted aluminum alloy for 30 min to prepare the $TiAl_3$/A356 composite. Next, UVT was applied to the melt. A structure diagram of the ultrasound device used in the experiment is shown in Fig.1. When the melt was cooled down to 620 °C, the horn and treatment furnace were kept at the same temperature for heat preservation, since the ultrasonic horn needed to be immersed in the melt. The ultrasonic generator was turned on at five different temperatures: 615, 608, 600, 593 and 586 °C, i.e. at five different solid fraction, 0.17, 0.28, 0.37, 0.44, 0.49. The powers of the ultrasonic generator were set to 400, 600, 800 W, and 1 kW at a frequency of 20 kHz. During the UVT, the melt was cooled in the furnace at a rate of about 8 °C /min. The UVT was applied for different time (0~180 s). The composite slurry was drawn with quartz straw and then cooled sample was could immediately with water. Specimens with diameter of 22 mm for the metallographic examination were cut from the quenched rods, then polished and etched by solution with solution of 0.5 vol% HF acid in ethanol for 10 s. The microstructures were examined using an optical microscope (OLYMPUS PMG-3), and micrographs of the samples were analyzed by a digital image analyzer system (Image-Pro Plus 6.0). The average diameter measured in a particle was defined as the size of the particle since its shape is irregular. The average diameter and shape coefficient (R_n) of primary α-Al particle in this study were defined as:

$$d = 2\sqrt{\frac{A}{\pi}} \quad (2)$$

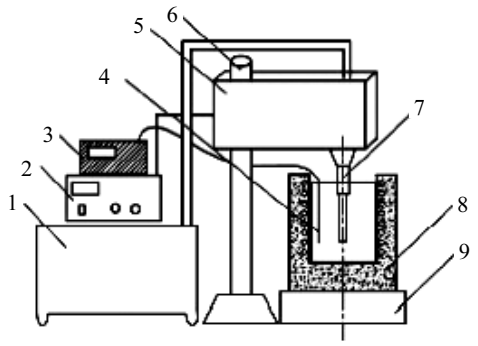

1 Cooling water tank and pipeline, 2 Ultrasonic generator, 3 Temperature controller, 4 Thermocouple, 5 Ultrasonic transducer, 6 Elevating bar, 7 Ultrasonic horn, 8 Resistance furnace, 9 Supporting disk

Fig.1 Schematic diagram of UVT device

$$R_n = \frac{4\pi A}{P^2} \quad (3)$$

where A and P are the area and the perimeter of the primary α-Al particles. In order to obtain the average size and shape coefficient of solid particles more accurately, more than 100 particles were measured in each sample.

2 Results and Discussion

2.1 Microstructures of $TiAl_3$/A356 composites

The XRD pattern of the $TiAl_3$/A356 composite prepared by UVT with a power of 1 kW at 608 °C for 60 s is shown in Fig.2. In addition, the peaks for $TiAl_3$ can be found as well as those for Al and Si. It proves that $TiAl_3$ is synthesized in the composite slurry.

The $TiAl_3$ particles formed block shapes are shown in Fig.3. Without UVT, a majority of primary α-Al particles exhibit coarse dendrites with lengths of 200 μm (Fig. 3a). When treated for 60 s, spheroids and rosette-shaped primary α-Al particles with an average size of 70 μm are observed (Fig.3b). The microstructure changes of primary α-Al particles were mainly due to the acoustic streaming and cavitation induced by UVT. During the UVT period, cavitation may produce numerous ‘micro-bubbles’. These ‘micro-bubbles’ expanded and burst, leading to sudden increase in local pressure and local undercooling. ‘Micro-bubbles’ became nucleation cores, increasing the nucleation rate. Furthermore, the burst of ‘micro-bubbles’ induced high-pressure shock waves and jets, leading to a dendrite fragmentation and accordingly refining grains. However, the effect of acoustic streaming led to a homogeneous distribution of temperature, which indicate a higher constitutional undercooling. Therefore, the morphology of primary α-Al particle may become finer and more rounded.

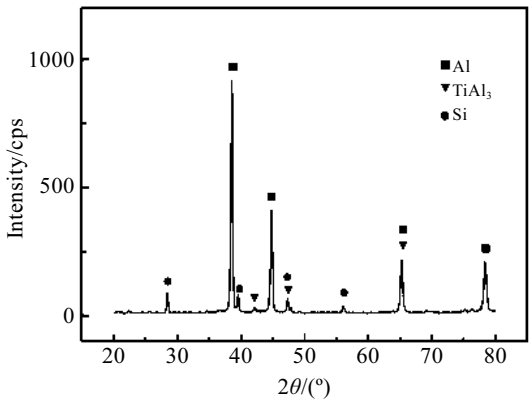

Fig.2 XRD pattern of semi-solid slurry of $TiAl_3$/A356 Composite

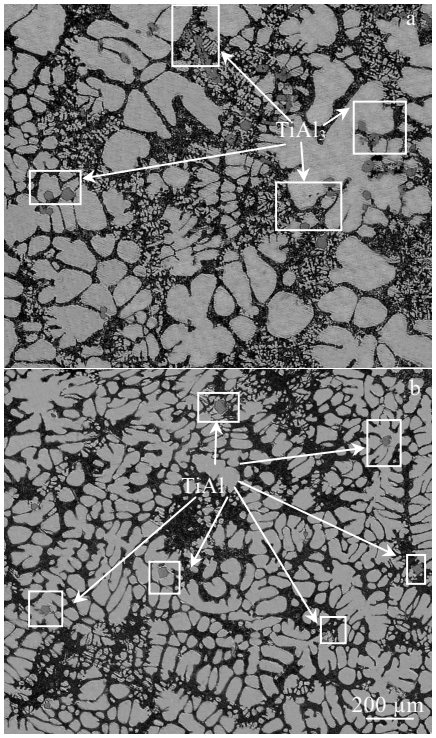

Fig.3 Microstructures of semi-solid slurry of $TiAl_3$/A356 composite at 608 °C: (a) without UVT, (b) with a UVT power of 1 kW treated for 60 s

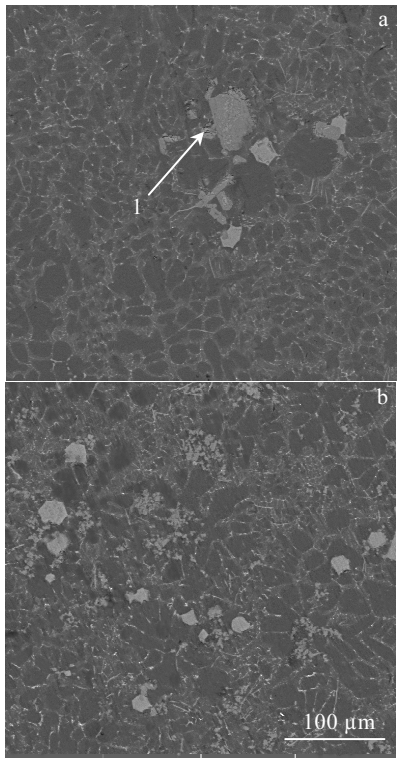

Fig.4 SEM micrographs of semi-solid slurry of $TiAl_3$/ A356 composite without UVT (a), with UVT (b) at 608 °C for 60 s

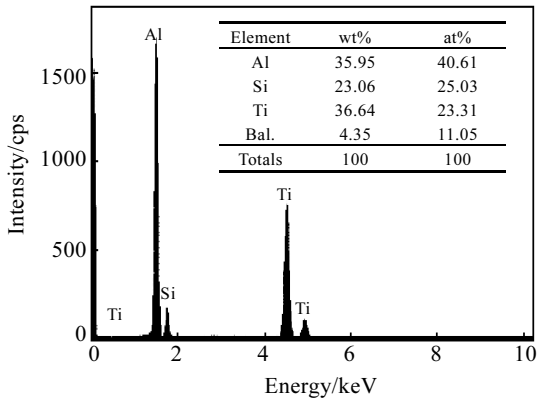

Fig.5 EDS spectrum of arrow 1 in Fig.4a

To corroborate the synthesizing of $TiAl_3$ in the composite, EDS result of the blocky particle in Fig.4b is shown in Fig.5. According to the EDS result, the blocky particle is $TiAl_3$. Before applying UVT, $TiAl_3$ particles are characterized by block and plate shapes, while few of them presented short stick shapes in Fig.4a. $TiAl_3$ particle size is large with a maximal size of approximately 80 μm. Furthermore, there is an obvious agglomeration of $TiAl_3$ particle. After applying UVT, the $TiAl_3$ particle decreases to a size of approximately 20 μm. In addition, the agglomeration is significantly decreased and $TiAl_3$ particles are uniformly distributed in the composite slurry. It indicates that the synthesized $TiAl_3$ particles can be the more uniformly dispersed into the melt due to the high pressure produced by acoustic streaming and cavitation. Moreover, the large $TiAl_3$ particles are also broken up by the high-pressure shock waves and jets generated by the bubble burst, so that the size of the $TiAl_3$ particles decreases.

2.2 Effect of UVT temperature

The microstructures of semi-solid slurry of $TiAl_3$/A356 composites produced at different UVT temperatures are shown in Fig.6. It is clear that some more round and finer primary α-Al particles were generated in the composite slurry when the UVT temperature is 615 °C (Fig. 6a). Here, the melt temperature of 615 °C is relatively high and the solid fraction is 0.17. The number of primary α-Al particle is less and the size becomes small. When treated at 608 °C (Fig. 6b), the primary α-Al particle number significantly increases and most of the primary α-Al particles exhibit spherical shapes. However, some individual primary α-Al particles increase in size. When treated at 600 °C (Fig. 6c), the number and size of rosette primary α-Al particles increase. When treated at 593 °C (Fig. 6d), the primary α-Al particle change significantly. The shape of most primary α-Al particle change to rosette with roundness decrease and size significantly increases.

To obtain the changes in size and morphology of primary α-Al particles more intuitively, the primary α-Al particle size and shape coefficient were measured when treated at 1 kW for 60 s. The results are show in Fig. 7. With the decrease of UVT temperature, the size gradually increases, the shape coefficient increases at first and then decreases. When treated at 600 °C or lower, the size significantly increases, and the shape coefficient significantly decreases. When treated at 608 °C, the shape coefficient reached a maximal of about 0.8. The higher the shape coefficient, the more round the particle. It indicates that semi-solid microstructure with a more rounded shape and a smaller size can be obtained. When the UVT temperature is high, the solid fraction is low, and the primary α-Al particles are less, and the effect of UVT on the semi-solid microstructure is minor. Therefore, the morphology of the microstructure is ordinary. When the UVT temperature is low, the solid fraction is high and the primary α-Al particle size is large. Consequently, the flow resistance of composite slurry increased, leading to the attenuation of the UVT effect. It is not conducive to breaking dendrite or dispersed primary α-Al particles. Therefore, the primary α-Al particle size is large and the morphology is suboptimal.

2.3 Effect of UVT time

The microstructures of semi-solid slurry of $TiAl_3$/A356 composite treated for different time are shown in Fig.8. When treated for 30 s (Fig. 8a), the primary α-Al particle is characterized by a rosette or an ellipse. Because of the short UVT time, the dendrite is too late to be broken by acoustic streaming. The growth of particle is not severely affected and the particle morphology is suboptimal. When treated for 60 s (Fig. 8b), as can be seen, the primary α-Al particle are rounded and almost become spherical. At this point, the effect of UVT on the microstructure change is optimal. The and the shape coefficient decreases as the UVT time (90 and 180 s) increases. This is mainly because the primary

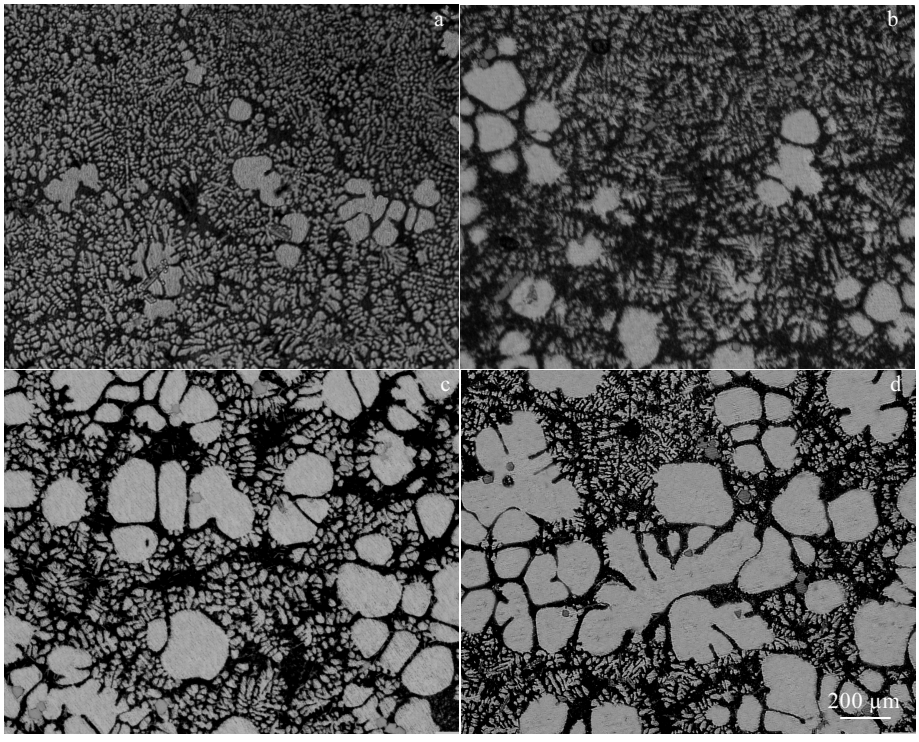

Fig. 6 Microstructures of semi-solid slurry of $TiAl_3$/A356 composite prepared by UVT with a power of 1 kW for 60 s at 615 °C (a), 608 °C (b), 600 °C (c), 593 °C (d)

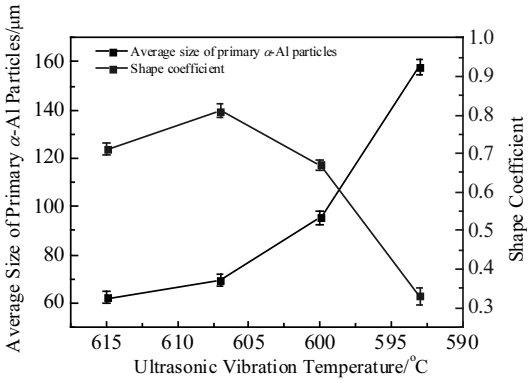

Fig. 7 Effect of UVT temperature on average size and shape coefficient of primary α-Al particles prepared by UVT at 1 kW for 60 s

dendrite could be fully broken by acoustic streaming and the semi-solid composite microstructures are uniformly dispersed. Therefore, the morphology is good. When treated for 90 s (Fig. 8c), the size of primary α-Al particle increases with the appearance of more rosette dendrites. When treated for longer time (180 s), the primary α-Al particle size evidently increases and a lot of rosette dendrites appear (Fig. 8d).

The relationships among the UVT time and the primary α-Al particle average size and shape coefficient are shown in Fig.9. At the beginning of the UVT (30~60 s), the average particle size decreases slightly and the shape coefficient increases. After treated for 60 s, the average size of the primary α-Al particle is minimal with 74 μm. The primary α-Al particle morphology is optimal and the shape coefficient is approximately 0.7. The particle size increases

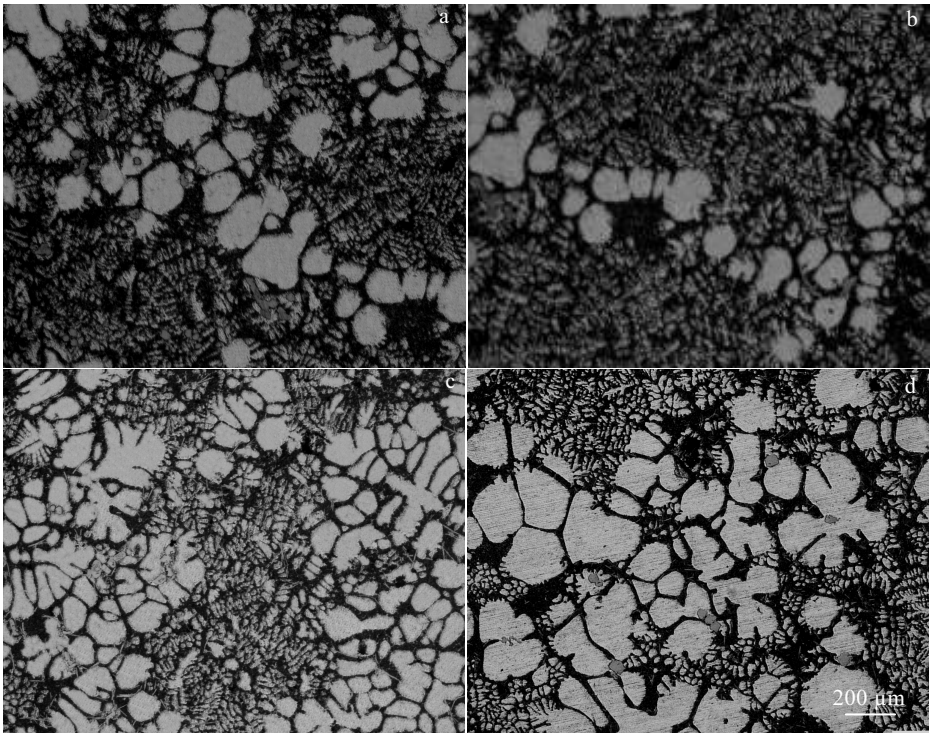

Fig. 8 Microstructures of semi-solid slurry of $TiAl_3$/A356 composite prepared by UVT with a power of 1 kW at 608 °C for 30 s (a), 60 s (b), 90 s (c),and 180 s (d)

and the shape coefficient decreases as the UVT time (90 and 180 s) increases. This is mainly because the primary α-Al particle size increases as the solid fraction increases. Thus, the flow resistance of composite slurry increases, leading to the attenuation of the UVT effect. However, the primary α-Al particle number increases, making the primary α-Al particle easier to aggregate and grow. Therefore, the primary α-Al particle size and morphology are suboptimal.

2.4 Effect of UVT power

The microstructures of semi-solid slurry of $TiAl_3$/A356 composites under different UVT powers are shown in Fig. 10. When the UVT power is 400 W (Fig. 10a), the primary α-Al particles appear as a larger size dendrite structure and sometimes there are a small number of more rounded primary α-Al particles. Furthermore, it could be observed that the large sized primary α-Al particles has dendrite fragmentation, indicating that some of the dendrite arms are broken. However, due to the low UVT power, the effect of UVT on the microstructure is not obvious. Some dendrites remained unbroken, and the morphology is poor.

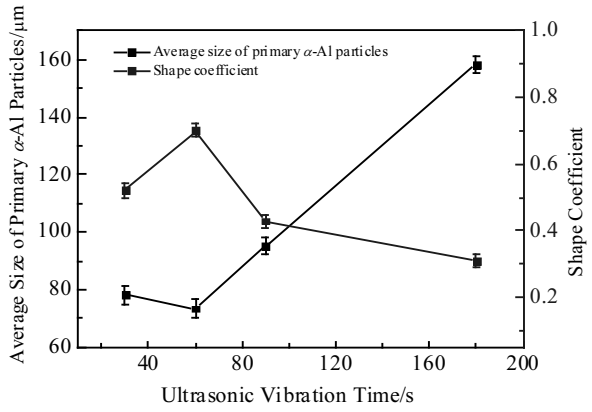

Fig.9 Effect of UVT time on average particle size and shape coefficient of primary α-Al particles prepared by UVT with a power of 1 kW at 608 °C

When the UVT power increases to 600 W (Fig. 10b), the effect of UVT on dendrite fragmentation is enhanced and the primary α-Al particle is elliptical and rosette-like. When a higher UVT power (800 W or 1 kW) is applied, the effect of acoustic streaming can fully break the dendrite and disperse the particles in the melt. Therefore, particles size and morphology are good (Fig. 10c and 10d). Furthermore, the primary α-Al particle number increases under high UVT power. At this stage, the effects of cavitation become apparent due to the high UVT power. There are numerous 'micro-bubbles' produced in the melt. These 'micro-bubbles' grew up, burst, and became the nucleation, leading to an increased nucleation rate. Therefore, the primary α-Al particle size is small. The changes in the primary α-Al particle average size and morphology under different UVT power are shown in Fig.11. With the UVT power increasing, the primary α-Al particle size gradually decreases, while the shape coefficient gradually increases. The dendrite is broken by the acoustic streaming effect, so the particle dispersion become more and more obvious, and the primary α-Al particle gradually changes from the dendrite, to rosette, which are almost spherical. The morphology of grains is gradually improved.

2.5 Discussion

The analysis of results reveals that the effect of UVT on the semi-solid microstructure is mainly caused by the cavitation and acoustic streaming. When treated by UVT in the melt, many tiny bubbles will be produced. The theory of cavitation is a series of dynamic processes of the expansion of 'micro-bubbles' [20,21], which was caused by the sound wave vibration. The acoustic streaming happened when the ultrasonic wave propagated in the melt. The sound pressure gradient in the direction of the sound wave propagation can be generated by the resistance of the sound wave in the melt, leading to circulation in the melt. Particularly, the morphology and size of particles were affected by UVT. The cavitation effect leads to an increase in the nucleation rate. The ultrasound leads to the fragmentation of the dendrite.

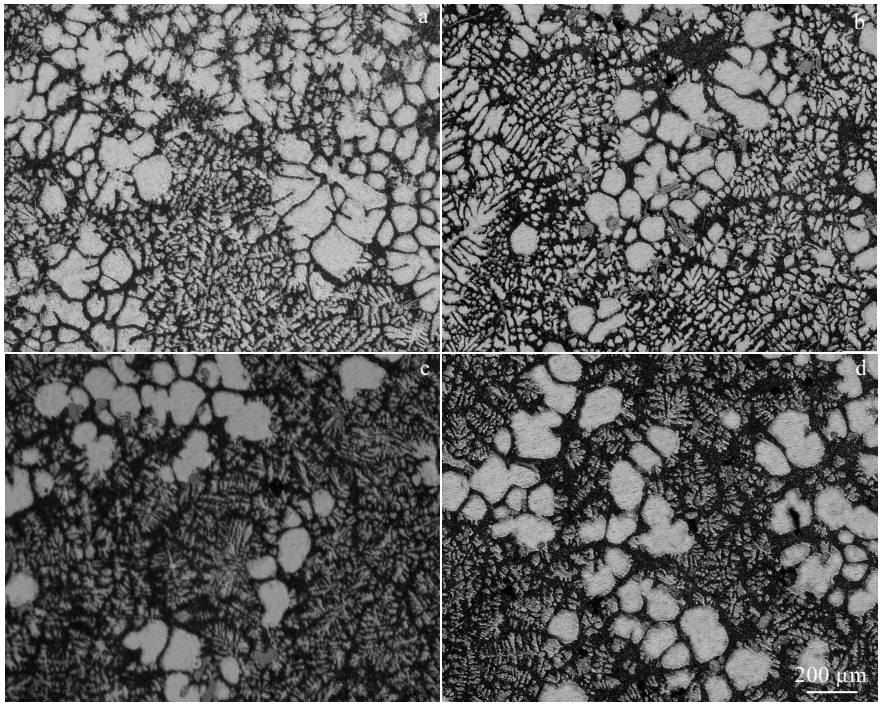

Fig.10 Microstructures of semi-solid slurry of $TiAl_3$/A356 composite prepared by UVT at 608 °C for 60 s with 400 W (a), 600 W (b), 800 W (c), and 1 kW (d)

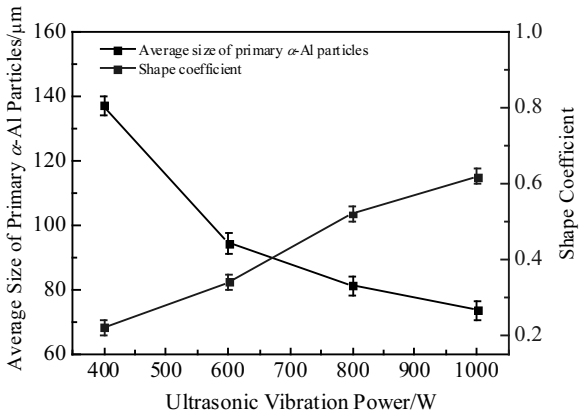

Fig.11 Effect of UVT power on average size and shape coefficient of primary α-Al particles prepared by UVT at 608 °C for 60 s

To produce a cavitation[22,23] effect, the UVT power has a specific strength. Only when the sound pressure is large enough to produce enough pressure in the melt, can the distance between the molecules in the melt reach or exceed the critical limit. Therefore, the melt structure can be destroyed, leading to the formation of the hole will be filled by the melt flow. When the hole was formed under the effect of sound waves, the cavitation occurred. The minimum sound pressure that causes the melt to produce a hole is called the cavitation valve. If the structure of the melt is complete (without defects), the threshold sound pressure can be calculated as:

$$P_{\mathrm{th}} = P_0 + 0.77\frac{\sigma}{R} \tag{4}$$

In Eq.(4), P_0 is the static pressure of the melt (a standard atmospheric pressure); σ is the surface tension coefficient of the melt; R is the radius of generated holes. σ is 0.860 N·m for aluminum. According to Eq.(4), it can be concluded that for a hole with a radius of 10 μm the threshold sound pressure $P_{\mathrm{th}} \approx 7.635\times10^5$ Pa. That means that at least 7.635×10^5 Pa of sound pressure are required to produce a hole with a radius of 10 μm. When applying UVT, the relationship between sound pressure and sound intensity can be described as:

$$P_{\mathrm{A}} = \sqrt{2I\rho c} \tag{5}$$

where P_{A} is the ultrasonic acoustic sound pressure produced by the ultrasonic wave; I is the ultrasonic acoustic sound intensity produced by the ultrasonic wave; ρ is the density of the melt, c is the propagation velocity of acoustic waves in the melt, and c is 5100 m/s for aluminum. The density of A356 is ρ = 2680 kg/m^3. Ultrasonic acoustic sound intensity can be described as:

$$I = P/\frac{\pi}{4}d^2 \tag{6}$$

In Eq.(6), P is the UVT power and d is the diameter of ultrasonic horn immersed in the melt. The diameter d of the ultrasonic equipment used in this experiment was 30 mm. The minimum UVT power was taken as 400 W, and the sound intensity was calculated as 5.662×10^5 W/m^2. The already calculated sound intensity was substituted into Eq.(4), resulting in a sound pressure generated by UVT of approximately 3.934×10^6 Pa for an UVT power of 400 W. In comparison, $P_{\mathrm{A}} > P_{\mathrm{th}}$. In this study, the smallest UVT power was 400 W. The liquidus temperature of the composite was 615 °C, so that in this study the highest UVT temperature was 615 °C. The lowest UVT temperature was 593 °C.

2.5.1 Effect of UVT temperature

According to Clausius-Clapeyron:

$$\Delta T_{\mathrm{m}} = \frac{T_{\mathrm{m}}\Delta P(V_{\mathrm{L}} - V_{\mathrm{S}})}{\Delta H} \tag{7}$$

In Eq.(7), ΔH is the latent heat of fusion, T_{m} is the melting point of metal, P is the pressure of the melt, and V_{L} and V_{S} are the volumes of the solid and liquid phases, respectively. We know that composites shrink and release heat during freezing. Therefore, it can se concluded that $\Delta H < 0$, $(V_{\mathrm{L}}-V_{\mathrm{S}}) < 0$. According to the increased pressure produced by a bubble burst, we know that $\Delta P > 0$. Therefore, we concluded that $\Delta T_{\mathrm{m}} > 0$ and the melting point increases. When the temperature is higher than 600 °C, the effective degree of undercooling increases, which promotes the nucleation of the melt and leads to an increase of nucleation rate to a certain extent. When UVT is applied at a lower temperature, there forms larger rosettes and irregular dendritic grains forms, which means the lower efficiency for UVT. Meanwhile, the agglomeration of particles is observed. Moreover, dendrite fragmentation induced by high-pressure shock waves and jets also played a role on the microstructure of dendritic α-Al particle. But with the temperature decreasing, the nucleation stage had already finished and solidification entered the growth stage. A large undercooling is needed for the free-growth activation of the finer $TiAl_3$ particles during solidification process. Furthermore, when the UVT applied below the liquidus temperature, the microstructure changes were mostly related to dendrite fragmentation induced by cavitation.

2.5.2 Effect of UVT time

When applying UVT for a short time (30 s), dendritic arms could not be fully broken and few ‘micro-bubbles’ expanded and burst. Cavitation and acoustic streaming had little influence on the morphology of particles. The increase in nucleation rate was not obvious. Thus, the microstructures of semi-solid composite slurry were rarely changed. The primary α-Al particles were characterized by

a rosette mixed with an ellipse and some coarse dendrites existed. When treated for 60 s, more 'micro-bubbles' rapidly expanded and burst. High-pressure shock waves and jets generated by the bursting of the bubble could fully break the dendritic arms. The nucleation rate increased, and cavitation and acoustic streaming did greatly affected the microstructure of composite slurry. The primary α-Al particles got more rounded and the shape coefficient increased. But with the UVT time getting longer (90 and 180 s), the solid fraction got higher. More solid volume of α-Al particles indicated a high opportunity of the solid particles contacting with each other, which led to the agglomeration of grains and lower vibration intensity. Hence, it was difficult to spheroidize and separate individual grains after agglomeration. Therefore, the shape coefficient decreased and the size of α-Al particles increased.

2.5.3 Effect of UVT power

When the UVT power is 400 W, the generated sound pressure exceeds the threshold sound pressure and can cause cavitation in the melt, producing cavitation bubbles. Energy around the melt is absorbed by the bubbles in the process of expansion, which leads to the local undercooling. Therefore, the bubble is the nucleation core. The relationship between the minimal radius of the cavitation bble and the sound pressure is as follows:

$$R^3_{\min} + \frac{2\sigma}{P_0} R^2_{\min} - \frac{32\sigma^{30}}{27(P_m - P_0)} = 0 \quad (8)$$

In Eq. (8), $R_{\min}$ is the minimum radius of the cavitation bubble; σ is the surface tension of the melt; P_m is the sound pressure amplitude; P_0 is the static pressure, σ and P_0 are constant. Therefore, the mathematical relationship can be deduced from the formula: the higher the P_m, the smaller the $R_{\min}$. This indicates that the number of cavitation bubbles increases for higher sound pressures. Eq. (5) and (6) reveal that the higher the UVT power, the higher both the ultrasonic intensity and sound pressure will be. The smaller the minimum radius of the bubble, the easier it will be to induce the cavitation effect, thus increasing the nucleation rate. The primary α-Al particles exhibit a more spherical shape, and the shape coefficient is larger and the morphology got better.

3 Conclusions

1) After applying of UVT, the $TiAl_3$ particles are evenly distributed in the semi-solid slurry of $TiAl_3$/A356 composite, and the particle size decreases. A good morphology of semi-solid composite with an average size of 62 μm and a shape coefficient of 0.8 can be obtained by applying UVT at 608 °C with a power of 1 kW for 60 s.

2) With the decrease of UVT temperature, the primary α-Al particle size gradually increases, and the primary α-Al particle morphology changes from a nearly spherical shape to an elliptical or rosette dendrite. With the increase of UVT time, the primary α-Al particle size decreases first and then increases. When the UVT time is 60 s, the primary α-Al particle morphology is optimal and the size becomes minimal. Further increasing the UVT time, the size of the particle increases and the shape coefficient decreases. With the increase of UVT power, the primary α-Al particle size decreases and the shape coefficient increases. When the UVT power is 1 kW, the primary α-Al particle size and morphology are better.

3) The mechanism of the microstructure development is the increase in the nucleation rate and undercooling caused by cavitation and acoustic streaming. Furthermore, in situ $TiAl_3$ particles have a lighter weight and a stronger direct bonding to the aluminum matrix composite.

References

1 Chen Z G, Ren J K, Zhang J S *et al. Rare Metal Materials & Engineering*[J], 2015, 44(10): 2341

2 Ma K K, Wen H M, Hu T *et al.* Acta Materialia[J], 2014, 62(5): 141

3 Xu F S, Guo X B, Wu P F *et al. Rare Metal Materials & Engineering*[J], 2017, 46(4): 0876

4 Kong D J, Wang J C, Liu H. *Rare Metal Materials & Engineering*[J], 2016, 45(5): 1122

5 Jian H G, Yin Z M, Jiang F *et al. Rare Metal Materials & Engineering*[J], 2014, 43(6): 1332

6 Qi X, Song R G, Qi W J *et al. Rare Metal Materials & Engineering*[J], 2016, 45(8): 1943

7 Zhou W W, Yamamoto G, Fan Y C *et al. Carbon*[J], 2016, 106: 37

8 Yuan L L, Han J T, Liu J *et al. Tribology International*[J], 2016, 98: 41

9 Xie B, Wang X G. *Rare Metal Materials & Engineering*[J], 2015, 44(5): 1057

10 Wang Z, Prashanth K G, Chaubey A K *et al. Journal of Alloys & Compounds*[J], 2015, 630: 256

11 Qi C, Wang J N, Lin Y H. *Bioresource Technology*[J], 2016, 211: 654

12 Zhao Jianhua, Shang Zhengheng, Wang Li *et al. Rare Metal Materials & Engineering* [J], 2015, 44(12): 3141 (in Chinese)

13 Kim J H, Lee K M, Lee H D *et al. Materials Transactions*[J], 2015, 56(3): 450

14 Chen X H, Yan H. *Materials & Design*[J], 2016, 94: 148

15 Zhang Junkai, Zhang Qin, Li Ying. *Rare Metal Materials & Engineering*[J], 2017, 46(1): 274 (in Chinese)

16 Zhang Yunpeng, Sun Guangbiao, Zhang Anzhou. *Rare Metal Materials & Engineering* [J], 2014, 43(1): 189 (in Chinese)

17 Huang W X, Yan H. *Journal of Rare Earths*[J], 2014, 32(6): 573

18 Chen X H, Yan H. *Journal of Materials Research*[J], 2015,

30(14): 2197
19 Yan H, Rao Y S, He R. *Journal of Materials Processing Technology*[J], 2014, 214(3): 612
20 Jiang R P, Li X Q, Zhang M. *Metals & Materials International*[J], 2015, 21(1): 104
21 Wan J, Yan H, Xu D. *International Journal of Materials Research*[J], 2015, 106(12)：1244
22 Liew P J, Yan J W, Kuriyagawa T. *International Journal of Machine Tools & Manufacture*[J], 2014, 76(1): 13
23 Lakshmanan P, Kalaichelvan K, Somakumar T. *Materials & Manufacturing Processes*[J], 2015, 31(10): 1275

超声振动法制备半固态 $TiAl_3$/A356 复合材料浆料的微观组织演变

孙勇辉[1]，闫 洪[1]，陈小会[2]，万 骏[1]，喻保标[1]
(1. 南昌大学，江西 南昌 330031)
(2. 新余学院，江西 新余 338004)

摘 要：利用超声振动法制备半固态 $TiAl_3$/A356 铝基复合材料浆料，利用扫描电镜和 X 射线衍射技术研究了超声温度，超声时间和超声功率对半固态 $TiAl_3$/A356 铝基复合材料浆料的微观组织的影响。结果显示，初生 α-Al 颗粒的尺寸随着超声温度和超声功率的降低而减小；随着超声时间的增加，先减小后增大。当超声温度为 608 ℃、超声功率为 1000 W、超声时间为 60 s 时，获得的半固态浆料组织中的初生 α-Al 颗粒形貌较为理想，平均初生 α-Al 颗粒尺寸为 62 μm，形状系数为 0.8。微观组织演变的机理是空化效应和声流效应引起的形核率和过冷度的增加。此外，原位生成的 $TiAl_3$ 颗粒有很强的结合 α-Al 颗粒的能力。

关键词：微观组织；半固态；铝基复合材料；超声振动；初生 α-Al 颗粒

作者简介：孙勇辉，男，1994 年生，硕士，南昌大学机电工程学院材料加工工程系，江西 南昌 330031，电话：0791-83969633，E-mail: 1446258442@qq.com